

# Carmeli's cosmology fits data for an accelerating and decelerating universe without dark matter nor dark energy

**Firmin J. Oliveira**

Joint Astronomy Centre Hilo, Hawai'i 96720

*firmin@jach.hawaii.edu*

**John G. Hartnett**

School of Physics, the University of Western Australia,

35 Stirling Hwy, Crawley 6009 WA Australia

*john@physics.uwa.edu.au*

January 25, 2020

## Abstract

A new relation for the density parameter  $\Omega$  is derived as a function of expansion velocity  $v$  based on Carmeli's cosmology. This density function is used in the luminosity distance relation  $\mathcal{D}_L$ . A heretofore neglected source luminosity correction factor  $(1 - (v/c)^2)^{-1/2}$  is now included in  $\mathcal{D}_L$ . These relations are used to fit type Ia supernovae (SNe Ia) data, giving consistent, well behaved fits over a broad range of redshift  $0.1 < z < 2$ . The best fit to the data for the local density parameter is  $\Omega_m = 0.0401 \pm 0.0199$ . Because  $\Omega_m$  is within the baryonic budget there is no need for any dark matter to account for the SNe Ia redshift luminosity data. From this local density it is determined that the redshift where the universe expansion transitions from deceleration to acceleration is  $z_t = 1.095^{+0.264}_{-0.155}$ . Because the fitted data covers the range of the predicted transition redshift  $z_t$ , there is no need for any dark energy to account for the expansion rate transition. We conclude that the expansion is now accelerating and that the transition from a closed to an open universe occurred about 8.54 Gyr ago.

Keywords: Carmeli's cosmology, high redshift type Ia supernovae, density parameter, dark matter

## 1 Introduction

Carmeli's cosmology, also referred to as cosmological general relativity (CGR), is a space-velocity theory of the expanding universe. It is a description of the

universe at a particular fixed epoch of cosmic time  $t$ . In CGR time is measured from the present back toward the big bang. At the present epoch  $t = 0$ , the universe can be described by its space-velocity “phase space” coordinates  $(v, r, \theta, \phi)$ . It is based on the Hubble law which says that the observed redshift  $z$  in the light emitted from a distant source of atoms is directly proportional to the distance  $D$  to the source, viz.  $v = H_0 D$ , where  $H_0$  is Hubble’s constant. CGR incorporates this basic law into a general 4D Riemannian geometrical theory satisfying the Einstein field equations (Ref. [2], appendix A).

This paper concerns itself with the average matter density  $\rho$  of the universe, or its normalised form, the density parameter  $\Omega$ . The density is the average mass per unit volume at a particular expansion velocity  $v$ . We derive a relation for  $\Omega$  and then use it in the luminosity distance relation  $\mathcal{D}_L$  to fit redshift distance modulus data from several high  $z$  type Ia supernovae (SNe Ia) experiments. This gives us an estimate of the density parameter  $\Omega_m$  at the present epoch. Additionally, we determine the redshift  $z_t$  at which the expansion rate makes the transition from decelerating to accelerating and the cosmic time  $t_t$  of the transition.

## 2 Density model

In terms of the phase space expansion history, the universe at the expansion velocity  $v$  has a total relativistic mass  $M$  and a total volume  $V$ . The expansion is assumed to be symmetric so that the volume  $V$  is spherical. The average matter density  $\rho$  is the ratio of the mass  $M$  to the volume  $V$ ,

$$\rho = \frac{M}{V}. \quad (1)$$

The total relativistic mass of matter

$$M = \frac{M_0}{\sqrt{1 - (v/c)^2}}, \quad (2)$$

where the expansion velocity  $v$  is assumed to be the average velocity of the matter.  $M_0$  is the rest mass of the universe at the present epoch where distance  $r = 0$  and  $v = 0$ , and  $c$  is the speed of light in vacuo. This form for the mass  $M$  is consistent with the solution to the Einstein equations for CGR.

The volume is taken to be that of a sphere

$$V = \frac{4\pi}{3}R^3, \quad (3)$$

where  $R$  is the radius of the portion of the universe that just contains the mass  $M$ . In CGR, the distance  $r$  is measured from the observer at the present epoch to the source rather than the other way, eg. as is done in the Friedmann theory of cosmology. We assume that higher density corresponds to higher velocity and

that the volume decreases as velocity increases. The radius  $R$  of the universe is therefore taken to be

$$R = c\tau - r, \quad (4)$$

where the redshift distance relationship [5] is given by

$$r = c\tau \sinh \left[ (v/c) \sqrt{1 - \Omega} \right] / \sqrt{1 - \Omega}, \quad (5)$$

and where  $v$  is the velocity of the source (galaxy) relative to an observer at  $r = 0$ . The Hubble-Carmeli time constant  $\tau \approx H_0^{-1}$  is a universal constant, the same for all observers.

$R$  is defined this way so that for  $v = 0$ ,  $R(r = 0) = c\tau$  is the radius of the sphere of the universe that just contains the mass of matter  $M_0$ . We define the average matter density parameter

$$\Omega = \frac{\rho}{\rho_c}, \quad (6)$$

where  $\rho_c$  is the critical density defined by

$$\rho_c = \frac{3}{8\pi G \tau^2}, \quad (7)$$

where  $G$  is Newton's gravitation constant. An overall constraint is that, for  $\Omega \geq 0$ ,

$$1 + \frac{(1 - \Omega)}{c^2 \tau^2} r^2 > 0. \quad (8)$$

From (1)-(7) the function for  $\Omega$  is

$$\Omega = \frac{\Omega_m / \sqrt{1 - \beta^2}}{\left[ 1 - \sinh \left( \beta \sqrt{1 - \Omega} \right) / \sqrt{1 - \Omega} \right]^3}, \quad (9)$$

where

$$\Omega_m = \frac{\rho_m}{\rho_c}, \quad (10)$$

$$\rho_m = \frac{M_0}{(4\pi/3)(c\tau)^3}, \quad (11)$$

$$\beta = \frac{v}{c}, \quad (12)$$

where  $\rho_m$  is the average matter density at the current epoch.

Though we have used rather crude arguments to obtain the equation for  $\Omega$ , the final outcome is a good measure of the density as a function of the expansion velocity. To look at it in another way, start with the density  $\Omega_m$  at zero velocity and then express the fact that the density increases relativistically proportional to  $(1 - \beta^2)^{-1/2}$  and inversely proportional to the normalized volume element  $(1 - r/c\tau)^3$ , which again gives (9).

As a check of the first order approximation, for  $\beta \ll 1$ ,  $z \approx \beta$  and since  $\sinh(x) \approx x$  for small  $x$ , (9) can be written

$$\Omega \approx \frac{\Omega_m (1 + (1/2)\beta^2)}{(1 - \beta)^3}, \quad (13)$$

$$\approx \Omega_m (1 + z)^3. \quad (14)$$

In the Friedmann-Robertson-Walker cosmologies, the matter density parameter  $\Omega = \Omega_m (1 + z)^3$  for all  $z$  in a dust dominated spatially flat universe, but this is not the case in the present theory where the density varies more strongly than  $(1 + z)^3$ . This will produce significant results in the data analysis.

We point out that the above functional form for  $\Omega$  is transcendental. For fits to data, it is more convenient to have a regular function. Below, we use a second order approximation for  $\Omega$  which is briefly described in appendix (A).

### 3 Expansion transition redshift $z_t$

Since CGR is a velocity based theory, the velocity of the source relative to the observer is well defined, in principle; it is the velocity  $v$  of expansion at the source position  $r$  relative to the observer at the present epoch. The redshift  $z$  due to  $v$  is related by the special relativistic wavelength shift equation

$$1 + z = \sqrt{\frac{1 + \beta}{1 - \beta}}. \quad (15)$$

In CGR the expansion has three basic phases: decelerating, constant and finally accelerating, corresponding to density  $\Omega > 1$ ,  $\Omega = 1$ , and  $\Omega < 1$ , respectively [4]. What is the expected velocity and redshift of the transition from deceleration to acceleration? This phase shift occurs during the zero acceleration or coasting phase when  $\Omega = 1$ . Taking (9) to the limit  $\Omega \rightarrow 1$ , since  $\sinh(x) \approx x$  for small  $x$ , yields

$$\lim_{\Omega \rightarrow 1} \Omega = 1 = \frac{\Omega_m / \sqrt{1 - \beta_t^2}}{(1 - \beta_t)^3}, \quad (16)$$

which simplifies to

$$(1 - \beta_t)^3 \sqrt{1 - \beta_t^2} = \Omega_m. \quad (17)$$

Solving (17) for  $\beta_t$ , the predicted redshift  $z_t$  of the expansion transition is obtained from (15). The transition redshift will be used in the data analysis to determine whether or not the expansion has evolved from decelerating to accelerating.

## 4 Comparison with high-z type Ia supernovae data

The redshift distance relationship in CGR is given by (5)

$$\frac{r}{c\tau} = \frac{\sinh(\beta\sqrt{1-\Omega})}{\sqrt{1-\Omega}}, \quad (18)$$

where, from (15)

$$\beta = \frac{(1+z)^2 - 1}{(1+z)^2 + 1}, \quad (19)$$

and  $\Omega$  is evaluated from (36).

In order to compare (18) with the high redshift SNe Ia data from Riess *et al* [21], Astier *et al* [1] and Knop *et al* [15] the proper distance is converted to magnitude as follows.

$$m(z) = \mathcal{M} + 5 \log [\mathcal{D}_L(z; \Omega)], \quad (20)$$

where  $\mathcal{D}_L$  is the dimensionless “Hubble constant free” luminosity distance. Refer [19, 20]. Here

$$\mathcal{M} = 5 \log\left(\frac{c\tau}{Mpc}\right) + 25 + M_B + a. \quad (21)$$

The units of  $c\tau$  are  $Mpc$ . The constant 25 results from the luminosity distance expressed in  $Mpc$ . However,  $\mathcal{M}$  in (20) represents a scale offset for the distance modulus ( $m - M_B$ ). It is sufficient to treat it as a single constant chosen from the fit. In practice we use  $a$ , a small free parameter, to optimize the fits.

In CGR a luminosity decreases according to

$$L_0 = L(1 - \beta^2), \quad (22)$$

where  $L$  is the absolute luminosity of the source galaxy in the Friedmann-Robertson-Walker (FRW) theory and  $L_0$  is the absolute luminosity of the source galaxy in the CGR theory. See Appendix B for details.

This then modifies the form of the luminosity distance accordingly and hence  $\mathcal{D}_L$  in CGR is given by

$$\mathcal{D}_L(z; \Omega_m) = \frac{r}{c\tau} (1+z) (1-\beta^2)^{-1/2} \quad (23)$$

using (18), which is a function of  $\Omega_m$  and  $z$ .

The parameter  $\mathcal{M}$  incorporates the various parameters that are independent of the redshift,  $z$ . The parameter  $M_B$  is the absolute magnitude of the supernova at the peak of its light-curve and the parameter  $a$  allows for any uncompensated extinction or offset in the mean of absolute magnitudes or an arbitrary zero point. The absolute magnitude then acts as a “standard candle” from which the luminosity and hence distance can be estimated.

The value of  $M_B$  need not be known, neither any other component in  $\mathcal{M}$ , as  $\mathcal{M}$  has the effect of merely shifting the fit curve (23) along the magnitude axis.

However by choosing the value of the Hubble-Carmeli constant  $\tau = 4.28 \times 10^{17} \text{ s} = 13.58 \text{ Gyr}$ , which is the reciprocal of the chosen value of the Hubble constant in the gravity free limit  $h = 72.17 \pm 0.84$  (statistical)  $\text{km.s}^{-1}\text{Mpc}^{-1}$  (see Section 7.1)  $\mathcal{M} = 43.09 + M_B + a$ .

We have taken the data of three SNe Ia data sets and curved fitted to them. The data are drawn from Table 5 of Riess *et al* [21], Tables 8 and 9 of Astier *et al* [1], the Supernova Legacy Survey (SNLS), and Table 5 of Knop *et al* [15]. Various fits to these are shown in figs 1, 3 and 4. Fig 2 shows the residuals between the data and the best statistical curve fits for the three data sets. The fitting algorithm fits a least squares method using the supplied data, without any weighting by the published errors.

The fit to the data of Astier *et al* is not shown as it is similar to fig. 1. However we combined the data sets of Riess *et al* and Astier *et al* and found the best statistical fit to all those data. This is shown in fig. 4 along with the curve where  $\Omega_m = 0.263$ , which is the value that Astier *et al* quote for the average matter density at the current epoch.

Finally we take the residuals between the combined the data set of Riess *et al* and Astier *et al* and the best fit curve of fig. 4. This is shown in fig. 5, along with the curve that represents  $\Omega_m = 0.263$ .

## 5 Quality of curve fits

In order quantify the goodness of the least squares fitting we have used the  $\chi^2$  parameter which measures the goodness of the fit between the data and the theoretical curve assuming the two fit parameters  $a$  and  $\Omega_m$ . Hence  $\chi^2$  is calculated from

$$\chi^2 = \sum_{i=1}^N \frac{1}{\sigma_i^2} [(m - M)(z)_i - (m - M)(z_{obs})_i]^2, \quad (24)$$

where  $N$  are the number of data;  $(m - M)(z)$  are determined from (20) with fit values of  $a$  and  $\Omega_m$ ;  $(m - M)(z_{obs})$  are the observed distance modulus data at measured redshifts  $z_{obs}$ ;  $\sigma_i$  are the published magnitude errors. The values of  $\chi^2/N$  ( $\approx \chi^2_{d.o.f}$ ) are shown in Table I, calculated using published errors on the distance modulus data. In each case the best fit value of  $a$  is found for each value of  $\Omega_m$ .

Table I lists the  $\chi^2/N$  parameters determined for three values of  $\Omega_m$ , as well as the best fit values of  $\Omega_m$  determined using the Mathematica software package. The latter are indicated by the word ‘best’ in the table. In the latter case the best fits are only statistically determined and hence also the standard error. In all instances the best fit value was determined for the parameter  $a$ .

The average of the three best fit  $\Omega_m$  values was calculated from

$$\Omega_m^* = \sum_{i=1}^3 \frac{\Omega_{mi}}{\sigma_i^2} / \sum_{i=1}^3 \frac{1}{\sigma_i^2}, \quad (25)$$

where  $\Omega_{mi}$  and  $\sigma_i$  are the best fit values from the three individual data sets, listed in Table I. The resulting average is  $\Omega_m^* = 0.051 \pm 0.024$ .

This is to be compared to the result obtained from the combined data set of Riess *et al* and Astier *et al*. There the best statistical fit resulted in a value of  $\Omega_m = 0.0401 \pm 0.0199$ , which is consistent with  $\Omega_m^*$ , the result obtained by averaging the values of  $\Omega_m$  obtained from the three individual data sets.

Table I: Curve fit parameters

Data set	N		a	$\sigma(stat)$	$\Omega_m$	$\sigma(stat)$	$\chi^2/N$
Riess <i>et al</i>	185	best	0.257		0.021		1.34188
			0.268		0.042		1.32523
			0.278	0.025	0.0631	0.0303	1.32152
Astier <i>et al</i>	117	best	0.158		0.021		11.2656
			0.161	0.043	0.0279	0.0430	11.3199
			0.168		0.042		11.4533
			0.177		0.063		11.6919
Knop <i>et al</i>	63	best	0.265		0.021		1.67301
			0.2694		0.042		1.67036
			0.2699	0.0387	0.0442	0.0989	1.67027
			0.274		0.063		1.67032
Riess + Astier	302	best	0.219		0.021		6.70338
			0.228	0.018	0.0401	0.0199	6.99446
			0.229		0.042		7.02192
			0.239		0.063		7.32371
			0.304		0.263		10.0568

The differences in the relative magnitudes of the  $\chi^2/N$  values for each data set is primarily the result of the size of the published errors used in the calculation (24) in the Astier *et al* data set. From the residuals in fig. 2, for Astier *et al*, it is seen that the published errors are small in relation to the deviation from the fitted curve. Whereas in the other two sets (Riess *et al* and Knop *et al*) the error bars are more often overlapping the fitted curve. Hence it appears that Astier *et al* have underestimated the real errors in their data, which is also indicated by their large scatter but small errors.

Looking at the  $\chi^2/N$  values the minimum regions in each set overlap where  $\Omega_m = 0.042$ . This is then the region of the most probable value. This is consistent with a value of  $\Omega_m = 0.0401 \pm 0.0199$  as determined from the combined data set shown in fig. 4. Therefore no exotic dark matter need be assumed as this value is within the limits of the locally measured baryonic matter budget  $0.007 < \Omega_m < 0.041$  [13] where a Hubble constant of  $70 \text{ km.s}^{-1}\text{Mpc}^{-1}$  was assumed.

The data of figs 1 and 4 are not determined better than the arbitrary scale offset. However Knop *et al* attempted to remove all uncertainties by making all possible corrections from which an effective magnitude ( $m_{B_{eff}}$ ) was determined. See [15] for the details. Therefore the Knop *et al* data contain the absolute magnitude of the fiducial SN Ia. Initially it was assumed that  $M_B = -19.3$  and then  $a$  was optimized for the best fit. This resulted in an absolute magnitude of  $M_B + a = -19.030$  determined from the best fit assuming all other corrections have been taken into account in the determination of the residuals for those data.

## 6 Discussion

Looking at the curve fits of fig. 4 where the distance modulus vs redshift curves with both  $\Omega_m = 0.0401$  and  $\Omega_m = 0.263$  are shown, it is quite clear that using the Carmeli theory a universe with  $\Omega_m = 0.263$  is ruled out and hence also the need for any dark matter. This is even more obvious from the residuals shown in fig. 5. There the fit with  $\Omega_m = 0.0401$  is drawn along the  $\Delta(m - M) = 0$  axis and the fit with  $\Omega_m = 0.263$  is shown as a broken line. The highest redshift data clearly rules out such high matter density in the universe.

The best fit result of this paper,  $\Omega_m = 0.0401 \pm 0.0199$ , with a density function that is valid for all  $z$  over the range of observations, is also consistent with the result obtained by Hartnett [14]  $\Omega_m = 0.021 \pm 0.042$  but in this paper, with the improved density function, the  $1\sigma$  errors are significantly reduced.

With the best fit  $\Omega_m = 0.0401$ , the predicted expansion transition redshift from (15) and (17) is

$$z_t = 1.095^{+0.264}_{-0.155}. \quad (26)$$

This is about a factor of 2 greater than the fitted value reported by Riess *et al.*[21] of  $z_t = 0.46 \pm 0.13$ , which was from a best fit to the differenced distance modulus data, a second order effect. They used a luminosity distance relation assuming a flat Euclidean space (i.e.,  $\Omega_{total} = 1$ ) and fit the difference data with the deceleration parameter  $q(z) = (dH^{-1}(z)/dt) - 1$ .

In the present theory, the transition redshift  $z_t$  is inherently where the density parameter  $\Omega(z_t) = 1$ . Thus, the transition is determined simultaneously with the initial fit of  $\mathcal{D}_L$  to the data.

Moreover  $\Omega_m$  has been determined as a ‘Hubble constant free’ parameter because it comes from  $\mathcal{D}_L(z; \Omega_m)$ , which is evaluated from fits using (23). The latter is independent of the Hubble constant or more precisely in this theory  $\tau$  the Hubble-Carmeli time constant. Therefore  $\Omega_m$  should be compared with  $\Omega_b$  and not with  $\Omega_b h^2$ , where  $h$  is the Hubble constant as a fraction of  $100 \text{ km.s}^{-1} \text{Mpc}^{-1}$  and not to be confused with  $h = 1/\tau$  used in CGR and this paper.

Nevertheless the value of  $\Omega_b h^2 = 0.024$  from [22] and  $h = 0.7217$  (assuming a value of  $\tau^{-1} = 72.17 \text{ km.s}^{-1} \text{Mpc}^{-1}$ ) implies  $\Omega_b = 0.043$ , which is in good agreement with the results of this work. Yet caution must be advised as the problem of the analysis of the WMAP data has not yet been attempted within the framework of CGR.

## 7 Values of some key parameters

### 7.1 Hubble constant

Using the small redshift limit of (18) and the Hubble law at small redshift ( $v = H_0 r$ ) it has been shown [7] that the Hubble parameter  $H_0$  varies with redshift. If it applies at the low redshift limit it follows from the theory that at high redshift we can write

$$H_0 = h \frac{\beta \sqrt{1 - \Omega}}{\sinh(\beta \sqrt{1 - \Omega})}. \quad (27)$$

Therefore  $H_0$  in this model is redshift dependent, not constant and  $H_0 \leq h$ . Only  $h = \tau^{-1}$  is truly independent of redshift and constant. The condition where  $H_0 = h$  only occurs at  $z = 0$  and where  $\Omega \rightarrow 0$ .

By plotting  $H_0$  values determined as a function of redshift, using (27), it is possible to get an independent determination of  $h$ , albeit the noise in the data is very large. This is shown in fig. 6 with values calculated by two methods with the exception of one point at  $z = 0.333$ . See figure caption for details. The data, even though very scattered, do indicate a trending down of  $H_0$  with redshift.

Separate curve fits from (27), with  $h$  as a free parameter, have been applied to the two data sets, Tully-Fisher (TF) (the solid line) and SNe type Ia (the broken line) measurements. The former resulted in  $h = 72.47 \pm 1.95$  (statistical)  $\pm 13.24$  (rms)  $km.s^{-1}Mpc^{-1}$  and from the latter  $h = 72.17 \pm 0.84$  (statistical)  $\pm 1.64$  (rms)  $km.s^{-1}Mpc^{-1}$ . The rms errors are those derived from the published errors, the statistical errors are those due to the fit to the data alone. The SNe Ia determined value is more tightly constrained but falls within the TF determined value.

### 7.2 Mass of the universe

It is easily shown from (7), (10) and (11) that

$$\Omega_m = R_s/R_0, \quad (28)$$

where  $R_s = 2G M_0/c^2$  is the Schwarzschild radius if the present universe rest mass  $M_0$  is imagined to be concentrated at a point, and  $R_0 = c\tau$  is the present radius of the universe. From this we get the present universe rest mass

$$M_0 = \Omega_m \frac{c^3 \tau}{2G}, \quad (29)$$

which, with  $\Omega_m = 0.0401 \pm 0.0199$  gives

$$M_0 = (1.74 \pm 0.86) \times 10^{21} M_\odot. \quad (30)$$

Likewise, the average matter density (11)

$$\rho_m = (3.92 \pm 1.94) \times 10^{-31} \text{gm cm}^{-3}. \quad (31)$$

### 7.3 Time of transition from deceleration to acceleration

From Carmeli's cosmological special relativity [10] we get a relation for the cosmic time in terms of the redshift. In particular, in terms of  $z_t$  we have for the cosmic time  $t_t$  of the expansion transition from the present

$$t_t = \tau \frac{(1+z_t)^2 - 1}{(1+z_t)^2 + 1}. \quad (32)$$

For the above value of  $z_t$  and for the age of the universe  $\tau = 13.58$  Gyr we have

$$t_t = 8.54_{-0.662}^{+0.903} \text{ Gyr}. \quad (33)$$

Since the big bang ( $t^* = 0$ ), the transition cosmic time is  $t_t^* = \tau - t_t$ ,

$$t_t^* = 5.04_{-0.903}^{+0.662} \text{ Gyr}. \quad (34)$$

In Fig. 7 is a plot of the density for  $\Omega_m = 0.04$ . More than 8.54 Gyr ago the density was higher than the critical value ( $\Omega > 1$ .) Since the transition the density has become less than critical ( $\Omega < 1$ ). The fit to the SNe Ia data was accomplished without the need for any dark energy, usually associated with the cosmological constant. In CGR there is no cosmological constant although a value for it may be obtained by a comparison study [6, 14].

## 8 Conclusion

The analysis in this paper has shown that the most probable value of the local density of the Universe is  $\Omega_m = 0.040$ , which is consistent with the statistical fit determined average  $\Omega_m^* = 0.051 \pm 0.024$  from three separate data sets and  $\Omega_m = 0.0401 \pm 0.0199$  the best fit from a combined data set of two totaling 302 data. The fits used a density function with limited range and validity and did not take into account the published errors on the individual magnitude data. The fits to the data are consistent over the entire range of the available redshift data, from  $0.1 < z < 2.0$ , a result of the more accurate relation for  $\Omega$ , as well as the proper accounting of the increase in the source luminosity due to the factor  $(1 - \beta^2)^{-1/2}$ .

Since  $\Omega_m$  is within the baryonic matter density budget, there is no need for any dark matter to account for the SNe Ia redshift magnitude data. Furthermore, since the predicted transition redshift  $z_t = 1.095_{-0.155}^{+0.264}$  is well within the redshift range of the data, the expansion rate evolution from deceleration to acceleration, which occurred about 8.54 Gyr ago, is explained without the need for any dark energy.

The density  $\Omega_m < 1$  and the determination of the transition redshift  $z_t$  within the data support the conclusion that the expansion is now accelerating and that the universe is, and will remain open.

## A Second order approximation for $\Omega$

The form for  $\Omega$  in (9) is transcendental, which is not convenient for fitting. A second order approximation can be made by taking  $\sinh(x) \approx x + x^3/3!$ . With this approximation (9) becomes

$$\Omega \approx \Omega_2 = \frac{\Omega_m / \sqrt{1 - \beta^2}}{\left\{ 1 - \left[ \beta \sqrt{1 - \Omega_2} + \beta^3 (\sqrt{1 - \Omega_2})^3 / 3! \right] / \sqrt{1 - \Omega_2} \right\}^3}, \quad (35)$$

which simplifies to

$$\Omega_2 \left[ 1 - \beta - \frac{\beta^3}{3!} + \frac{\beta^3}{3!} \Omega_2 \right]^3 - \left( \Omega_m / \sqrt{1 - \beta^2} \right) = 0. \quad (36)$$

This is a quartic equation in  $\Omega_2$  and can be solved for  $\Omega_2$  as a function of  $\beta$  by standard methods.  $\Omega_2$  is shown in fig. 7 as the broken line where a matter density  $\Omega_m = 0.040$  was assumed. It is compared with  $\Omega$  given by the exact form (9).

## B Addendum

Remo Tilanus [23] questioned the meaning of equation (22) above and asked for an explanation of the physics behind the effect. It was then realized that the luminosity distance needed to be derived correctly for the Cosmological General Relativity (CGR) [2]. The following derives the expression for the luminosity distance in the Carmeli theory as well as the angular size and surface brightness.

## C Luminosity distance

Lets compare the photons that leave a distance source galaxy at time  $t$  located at  $r$  to their reception by the observer at the origin of coordinates  $r = 0$ . Therefore the timescale is measured backwards from the origin defined by  $t = 0$ . This analysis follows that of Narlikar [17] pages 114-117.

Suppose  $L$  is the total energy emitted per unit time during the epoch  $t$  (that is, in the rest frame of the source galaxy) to be received by the observer at time  $t = 0$ . Therefore we can write

$$dL = LI(\lambda)d\lambda \quad (37)$$

where  $I$  is its (normalized) intensity distribution – a function of wavelength.

Now consider a packet of photons that leaves the source in the wavelength range  $(\lambda_0/(1+z), \lambda_0 + \Delta\lambda_0/(1+z))$  where  $\lambda_0$  refers to the wavelength of the photons received by the observer. The factor of  $(1+z)$  results from the expansion of the universe between emission and reception. That is the packet of photons arrives at the observer in the wavelength range  $(\lambda_0, \lambda_0 + \Delta\lambda_0)$ . The packet leaves

the source between times  $t$  and  $t + \Delta t$ . However in CGR times at cosmological distances add according to a relativistic addition law, [8] when referred to the observer at  $t = 0$ . Hence instead of the time interval  $\Delta t$ , we get

$$\Delta t \rightarrow \frac{t + \Delta t}{1 + \frac{t \Delta t}{\tau^2}} - t = \Delta t \left\{ 1 - \frac{t^2}{\tau^2} \right\}. \quad (38)$$

Therefore we can write for the total energy that leaves the source galaxy in the time interval  $(t, t + \Delta t)$ ,

$$LI \left( \frac{\lambda_0}{1+z} \right) \frac{\lambda_0}{1+z} \Delta t \left\{ 1 - \frac{t^2}{\tau^2} \right\}. \quad (39)$$

The number of photons in the interval  $\lambda_0/(1+z)$  to  $\lambda_0 + \Delta\lambda_0/(1+z)$  are

$$\delta\mathcal{N} = LI \left( \frac{\lambda_0}{1+z} \right) \frac{\Delta\lambda_0}{1+z} \Delta t \left\{ 1 - \frac{t^2}{\tau^2} \right\} \frac{\lambda_0}{(1+z)ch}, \quad (40)$$

since the energy per photon is  $(1+z)ch/\lambda_0$ , where  $c$  is the speed of light and  $h$  is Planck's constant. To get the number of photons received per unit surface area we need to divide by the area of the sphere centered on the source galaxy. Thus number of photons per unit area is

$$LI \left( \frac{\lambda_0}{1+z} \right) \frac{\Delta\lambda_0}{(1+z)^2} \frac{\Delta t}{\Delta t_0} \left\{ 1 - \frac{t^2}{\tau^2} \right\} \frac{\lambda_0}{ch} \frac{1}{4\pi r^2}, \quad (41)$$

where the photons are received over the time interval  $(t_0, t_0 + \Delta t_0)$ . However

$$\frac{c\Delta t}{c\Delta t_0} = \frac{\lambda}{\lambda_0} = \frac{1}{1+z}. \quad (42)$$

Since each photon is received with energy  $ch/\lambda_0$  we multiply by this factor to get the apparent luminosity,  $\mathcal{F}$ , in a  $\Delta\lambda_0$  wavelength interval and (41) becomes

$$\mathcal{F}(\lambda_0) \Delta\lambda_0 = LI \left( \frac{\lambda_0}{1+z} \right) \frac{1}{(1+z)^3} \left\{ 1 - \frac{t^2}{\tau^2} \right\} \frac{1}{4\pi r^2} \Delta\lambda_0. \quad (43)$$

Finally we integrate the normalized intensity function in (43) over all wavelengths, which results in

$$\mathcal{F}_{bol} = \frac{L_{bol}}{(1+z)^2} \left\{ 1 - \frac{t^2}{\tau^2} \right\} \frac{1}{4\pi r^2} = \frac{L_{bol}}{4\pi \mathcal{D}_L^2}. \quad (44)$$

where  $L_{bol}$  is the absolute bolometric luminosity of the source galaxy. Therefore the luminosity distance  $\mathcal{D}_L$  in CGR is expressed as

$$\mathcal{D}_L = r(1+z) \left\{ 1 - \frac{t^2}{\tau^2} \right\}^{-1/2}. \quad (45)$$

This is the exact expression used above, which was found to fit the observed data very well. Further discussion on the quality of the fits appears below in section F.

This means (keeping subscripts consistent with the above) that we can write

$$L_0 = L \left\{ 1 - \frac{t^2}{\tau^2} \right\}, \quad (46)$$

where  $L$  is the absolute luminosity of the source galaxy in the Friedmann-Robertson-Walker (FRW) theory and  $L_0$  is the absolute luminosity of the source galaxy in the CGR theory. Obviously as  $t \rightarrow 0$  at the present epoch,  $L_0 \rightarrow L$ . Therefore the effect we observe is a relativistic time dilation effect resulting from the cosmological transformation (in (38)) specific to the Carmeli theory. It is then clear that the expression (45) for the luminosity distance in CGR when compared to that in the FRW theory has this extra factor  $(1 - t^2/\tau^2)^{1/2}$ . Hence we expect the luminosity distance to be greater in CGR than in FRW theory.

## D Angular size

In the CGR the proper distance  $r$  in spherically symmetric coordinates is determined from (18). There is no scale factor like in the FRW theory but we can similarly define an expansion factor as  $(1+z)^{-1}$ . If we then make the substitution for the matter density  $\Omega = \Omega_m(1+z)^3$ , where  $\Omega_m$  is the matter density at the current epoch, the proper distance (18) can be rewritten as a function of  $(1+z)$ ,

$$r = c\tau \sinh \left( \beta \sqrt{1 - \Omega_m(1+z)^3} \right) / \sqrt{1 - \Omega_m(1+z)^3}. \quad (47)$$

For a proper comparison with FRW theory we must use the FRW equivalent of  $r/(1+z)$ , which is the Hubble distance  $D_1$  when the light we observe left the galaxy at redshift  $z$  and is given by

$$D_1 = \frac{2cH_0^{-1}}{(1+z)} \left\{ 1 - \frac{1}{\sqrt{1+z}} \right\}, \quad (48)$$

where a deceleration parameter  $q_0 = 1/2$  has been used. The angular size of the source galaxy in FRW theory is

$$\Delta\theta = \frac{d}{D_1}, \quad (49)$$

where  $d$  is the actual diameter of the source galaxy and the angular distance  $D_1$  is taken from (48).

In CGR the angular distance  $\mathcal{D}_A$  is defined identically with (49)

$$\Delta\theta = \frac{d}{\mathcal{D}_A}, \quad (50)$$

where the functional form for  $\mathcal{D}_A$  is determined by its relationship to the luminosity distance  $\mathcal{D}_L$ . To show how  $\mathcal{D}_L$  and  $\mathcal{D}_A$  are related we look at the flux  $F_\theta$  from a distant source of extent  $d$  which subtends an angle  $\Delta\theta$  on the sky [18]

$$F_\theta = \Delta\theta^2 \sigma T_o^4, \quad (51)$$

where  $\sigma$  is the Stephan-Boltzmann constant and  $T_o$  is the observed temperature of the source. Equating fluxes from (44) and (51), substituting for  $\Delta\theta$  from (50) and substituting  $L_{bol} = 4\pi d^2 \sigma T_e^4$  with  $T_e$  the source temperature we get

$$\frac{T_e^4}{\mathcal{D}_L^2} = \frac{T_o^4}{\mathcal{D}_A^2}. \quad (52)$$

Since for a blackbody at temperature  $T$  the radiation with average wavelength  $\lambda$  has energy  $h c / \lambda = kT$  where  $k$  is Boltzmann's constant and since the wavelength varies with redshift as  $(1+z)$  this implies  $T_o = T_e/(1+z)$ . We assume that this holds even for a galaxy source which may not be a perfect blackbody. Then (52) simplifies to

$$\mathcal{D}_L = \mathcal{D}_A (1+z)^2. \quad (53)$$

This relation is the same as that for FRW. Hence the angular size of a source galaxy in CGR can be found

$$\Delta\theta = \frac{d}{\mathcal{D}_A} = \frac{d(1+z)}{r} \left\{ 1 - \frac{t^2}{\tau^2} \right\}^{1/2}, \quad (54)$$

where (45) and (53) have been used.

Substituting (47) in (54) produces gravitational effects on the angular size that can be called lensing, and are clearly non-Euclidean. We have plotted in Fig. 8 the dependence of angular size  $\Delta\theta$  on redshift  $z$  for CGR using (47) in (54) but instead with the density function  $\Omega(z)$  determined above. That density expression replaces the simple form in (47) and better characterizes the universe at high redshifts.

In order to compare theories independently of the constants  $d$ ,  $c$  and  $\tau \approx H_0^{-1}$ , we plot  $\Delta\theta(z)/\Delta\theta(0.01)$  for both FRW and CGR theories. It is quite clear from Fig. 8 that for redshifts  $z \leq 0.2$  the two models are in reasonable agreement but in general  $\Delta\theta_{FRW} \neq \Delta\theta_{CGR}$ . For  $z > 0.2$  the details depend heavily on the parameters of the models chosen.

## E Surface brightness

To determine the effect of redshift variation on apparent surface brightness of a source we need to calculate the apparent brightness per unit angular surface area. It follows from (44), (53) and (54) that brightness per unit area,  $B$  is related by

$$B = \frac{\mathcal{F}_{bol}}{(\pi/4)\Delta\theta^2} = \frac{L_{bol}}{(\pi^2 d^2)(1+z)^4} \propto (1+z)^{-4}, \quad (55)$$

which is the same as the usual FRW expression, the same  $(1+z)^{-4}$  dependence Tolman [24] produces using standard cosmology.

## F Discussion

In the above we presented the parameter  $\chi^2/N$  as representative of the quality of the fits. Also I did the same in an earlier paper [14] to some of the same data but with a different density model. In the latter the  $\chi^2/N$  parameters appear to be much smaller and therefore represent better quality fits than in the former. However this is not actually the case. In the latter paper [14] a software algorithm was used that didn't properly calculate  $\chi^2$ . It should be calculated from (24) where  $\sigma_i$  are the published magnitude errors. The problem with the earlier software was that it automatically set the errors  $\sigma_i = 1$  for all data. I was not aware of this software problem at the time but in the we directly calculated the correct  $\chi^2/N$  parameters.

The values of  $\chi^2/N$  ( $\approx \chi^2_{d.o.f.}$ ) are here again shown in Table II for the combined data set of Riess *et al* and Astier *et al*, calculated using published errors on the distance modulus data. In each case the best fit value of  $a$  is found for each value of  $\Omega_m$ . For comparison I have also tabulated in Table II the  $\chi^2/N$  parameters where  $\sigma_i$  are forced to unity.

Table II: Curve fit parameters of combined data of Riess *et al* + Astier *et al*

a	$\sigma(stat)$	$\Omega_m$	$\sigma(stat)$	$\chi^2/N$	$\chi^2/N (\sigma_i = 1)$
0.219		0.021		6.70338	0.075039
0.228	0.018	0.0401	0.0199	6.99446	0.074726
0.229		0.042		7.02192	0.074728
0.239		0.063		7.32371	0.075010
0.304		0.263		10.0568	0.086165

The resulting  $\chi^2/N(\sigma_i = 1)$  are extremely good even compared to the 185 data of Riess *et al* fitted to in Fig. 1 of Hartnett [14] where  $\chi^2/N(\sigma_i = 1) = 0.2036$  was calculated. In fact, the  $\chi^2/N(\sigma_i = 1)$  are about 3 times smaller in the fits shown in Figs 1 and 4. Only the fits with much smaller numbers of data in Hartnett [14] show better  $\chi^2/N(\sigma_i = 1)$  values and in those cases the comparisons are not as valid because the number of degrees of freedom are generally much larger in the fits shown here.

The improvement has resulted from the refinement of the density model  $\Omega(z)$  and the additional factor  $(1 - t^2/\tau^2)^{-1/2}$  in the luminosity distance. If we exclude the new density model and use  $\Omega = \Omega_m(1 + z)^3$  where  $\Omega_m = 0.04$  instead, we get  $\chi^2/N(\sigma_i = 1) = 0.075986$  for the best fit to the combined data set requiring  $a = 0.2152$ . This indicates the improvement over Hartnett [14] is more the result of the additional factor in the luminosity distance than the better density model.

The larger values of  $\chi^2/N$  in column 5 in Table II is more indicative of the poorly determined errors on the measured magnitudes. They are in fact much worse in the Astier *et al* data set than in that of Riess *et al*.

Here it has been shown that luminosity distance in Cosmological General Relativity is greater by a factor of  $(1 - t^2/\tau^2)^{-1/2}$ . It also follows that the

surface brightness is the same as in standard cosmology, though angular size is smaller by a factor of  $(1 - t^2/\tau^2)^{1/2}$ .

## References

- [1] P. Astier, *et al* “The Supernova Legacy Survey: Measurement of  $\Omega_M$ ,  $\Omega_\Lambda$  and  $w$  from the first year data set”, *Astron. Astrophys.* (2005) arXiv:astro-ph/0510447
- [2] M. Carmeli, “Cosmological Special Relativity”, 2nd Ed., (World Scientific, Singapore, 2002)
- [3] ibid. pp. 117-124
- [4] ibid. pp. 125-127
- [5] ibid. p. 158
- [6] ibid. pp. 170-172
- [7] ibid. p. 159
- [8] ibid. Sec. 2.15.4, p. 23.
- [9] M. Carmeli, “Cosmological Relativity: Determining the Universe by the cosmological redshift as infinite and curved”, *Int. J. Theor. Phys.* **40**: 1871-1874 (2001)
- [10] M. Carmeli, J.G. Hartnett, F.J. Oliveira, “The cosmic time in terms of the redshift,” arXiv:gr-qc/0506079, *Found. Phys. Letters* (in press) (2005)
- [11] W.L. Freedman, B.F. Madore, J.R. Mould, R. Hill, L. Ferrarese, R.C. Kennicutt Jr, A. Saha, P.B. Stetson, J.A. Graham, H. Ford, J.G. Hoessel, J. Huchra, S.M. Hughes and G.D. Illingworth, “Distance to the Virgo cluster galaxy M100 from Hubble Space Telescope observations of Cepheids”, *Nature* **371**: 757-762 (1994)
- [12] W.L. Freedman, B.F. Madore, B.K. Gibson, L. Ferrarese, D.D. Kelson, S. Sakai, J.R. Mould, R.C. Kennicutt Jr, H.C. Ford, J.A. Graham, J.P. Huchra, S.M.G. Hughes, G.D. Illingworth, L.M. Macri, and P.B. Stetson, “Final results from the Hubble Space Telescope Key Project to measure the Hubble constant”, *Ap. J.* **553**:47-72, (2001)
- [13] M. Fukugita, C.J. Hogan, and P.J.E. Peebles, “The cosmic baryon budget”, *Ap. J.* **503**: 518-530 (1998)
- [14] J.G. Hartnett, “The distance modulus determined from Carmeli’s cosmology fits the accelerating universe data of the high-redshift type Ia supernovae without dark matter”, *Found. Phys.* **19**(2) (2006) (in press) arXiv:astro-ph/0501526.

- [15] R.A. Knop *et al* “New constraints on  $\Omega_M$ ,  $\Omega_\Lambda$  and  $w$  from an independent set of 11 high-redshift supernovae observed with the Hubble Space Telescope”, *Ap. J.* **598**: 102-137 (2003)
- [16] L.M. Krauss “The end of the age problem, and the case for a cosmological constant revisited”, *Ap. J.* **501**: 461-466 (1998)
- [17] J.V. Narlikar, “An Introduction to Cosmology”, 3rd Ed., (Cambridge University Press, Cambridge, 2002)
- [18] E.L. Wright, “Homogeneity and Isotropy; Many Distances; Scale Factor”, [http://www.astro.ucla.edu/~wright/cosmo\\_02.htm](http://www.astro.ucla.edu/~wright/cosmo_02.htm).
- [19] S. Perlmutter *et al* “Measurements of the cosmological parameters  $\Omega$  and  $\Lambda$  from the first seven supernovae at  $z > 0.35$ ”, *Ap. J.* **483**:565-581 (1997)
- [20] A.G. Riess, A. V. Filippenko, P. Challis, A. Clocchiatti, A. Diercks, “Observational evidence from supernovae for an accelerating universe and a cosmological constant”, *Astron. J.* **116**: 1009-1038 (1998)
- [21] A.G. Riess, *et al* “Type Ia supernovae discoveries at  $z > 1$  from the Hubble Space Telescope: Evidence for past deceleration and constraints on dark energy evolution” *Ap. J.* **607**: 665-687 (2004)
- [22] D. N. Spergel *et al* “Wilkinson Microwave Anisotropy Probe (WMAP) three year results: Implications for cosmology”, arXiv:astro-ph/0603449
- [23] R.P. Tilanus, Joint Astromony Centre, Hilo, Hawaii, U.S.A.
- [24] R.C. Tolman “On the estimation of distances in a curved universe with non-static line element”, Proc. Nat. Acad. Sci. **16**: 515-520, (1930)
- [25] Y. Tutui *et al*. (2001). PASJ. **53**: 701, arXiv:astro-ph/0108462

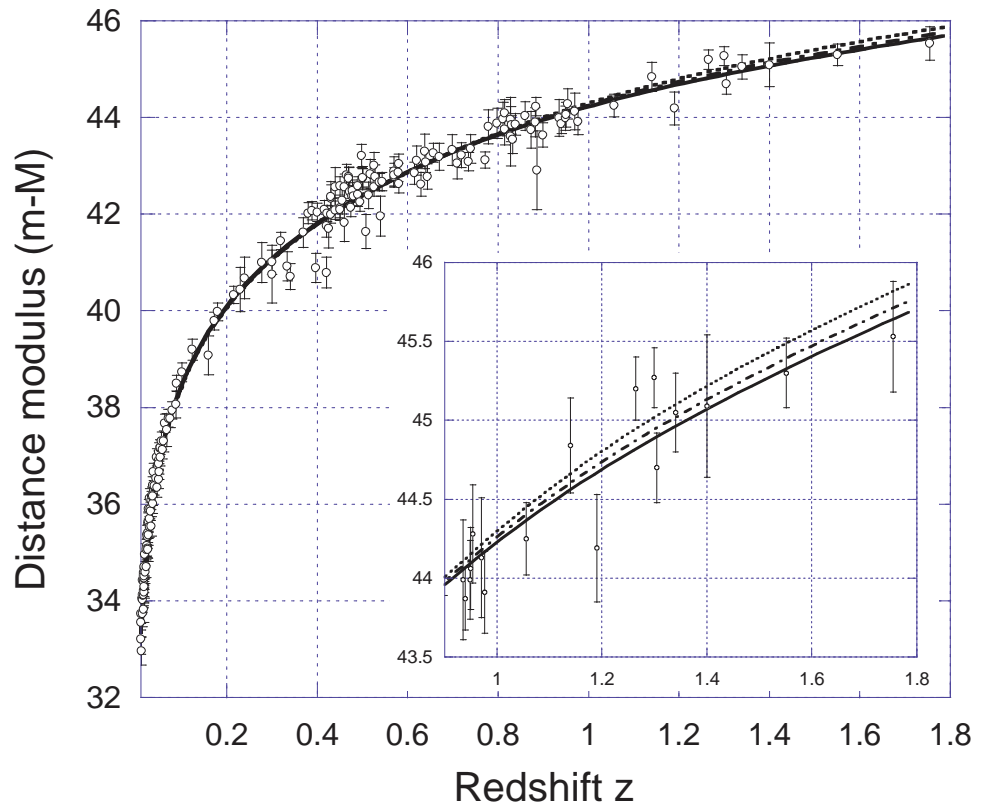


Figure 1: Data taken from Table 5 of Riess *et al* [21]. The solid line curve uses the best fit value of  $a$  with  $\Omega_m = 0.063$ , the dot-dash line curve uses the best fit value of  $a$  with  $\Omega_m = 0.042$  and the dotted line curve uses the best fit value of  $a$  with  $\Omega_m = 0.021$

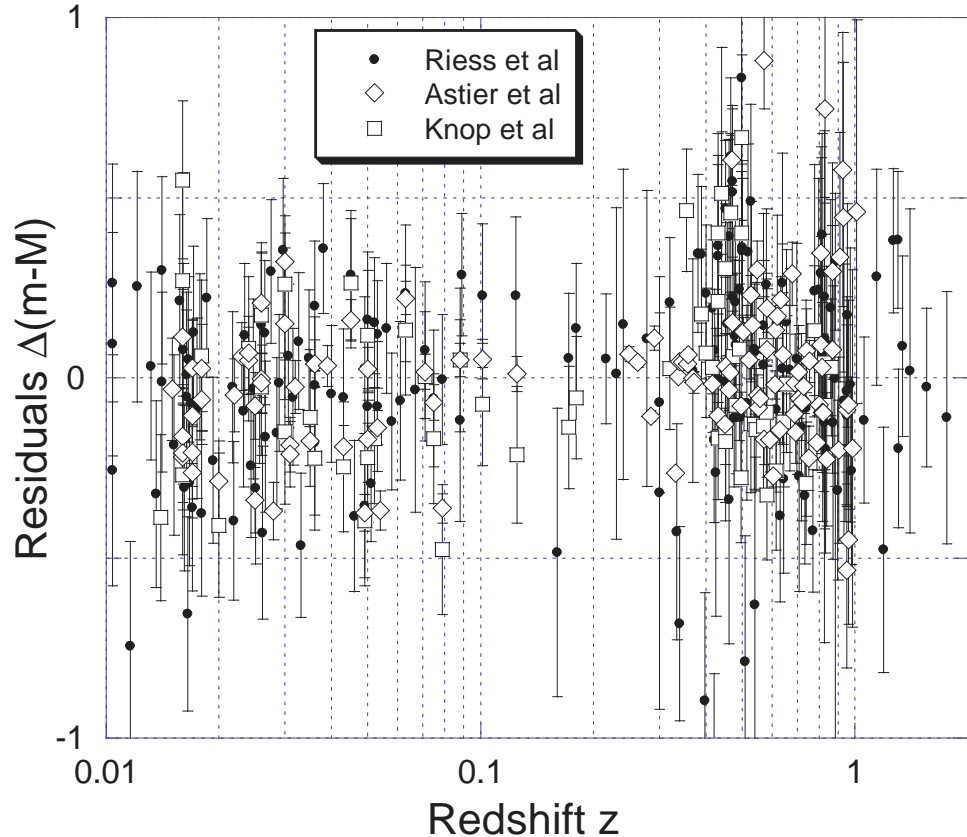


Figure 2: Residuals vs redshift (on log scale) for three data sets. 1) The solid dots are the differences between the curve with  $\Omega_m = 0.063$  and  $a = 0.278$  and the data of Riess *et al* [21] shown in fig. 1. The mean of these residuals is  $2.2 \times 10^{-5}$  when all errors are assumed equal and 0.0274 when weighted by published errors. 2) The open diamonds are the differences between the curve with  $\Omega_m = 0.028$  and  $a = 0.203$  and the data of Astier *et al* [1]. The mean of these residuals is  $3.74 \times 10^{-4}$  when all errors are assumed equal and  $-0.0177$  when weighted by published errors. 3) The open squares are the differences between the curve with  $\Omega_m = 0.044$  and  $a = 0.270$  and the data of Knop *et al* [15] shown in fig. 3. The mean of the residuals is  $9.92 \times 10^{-6}$  when all errors are assumed equal and  $-0.00515$  when weighted by published errors

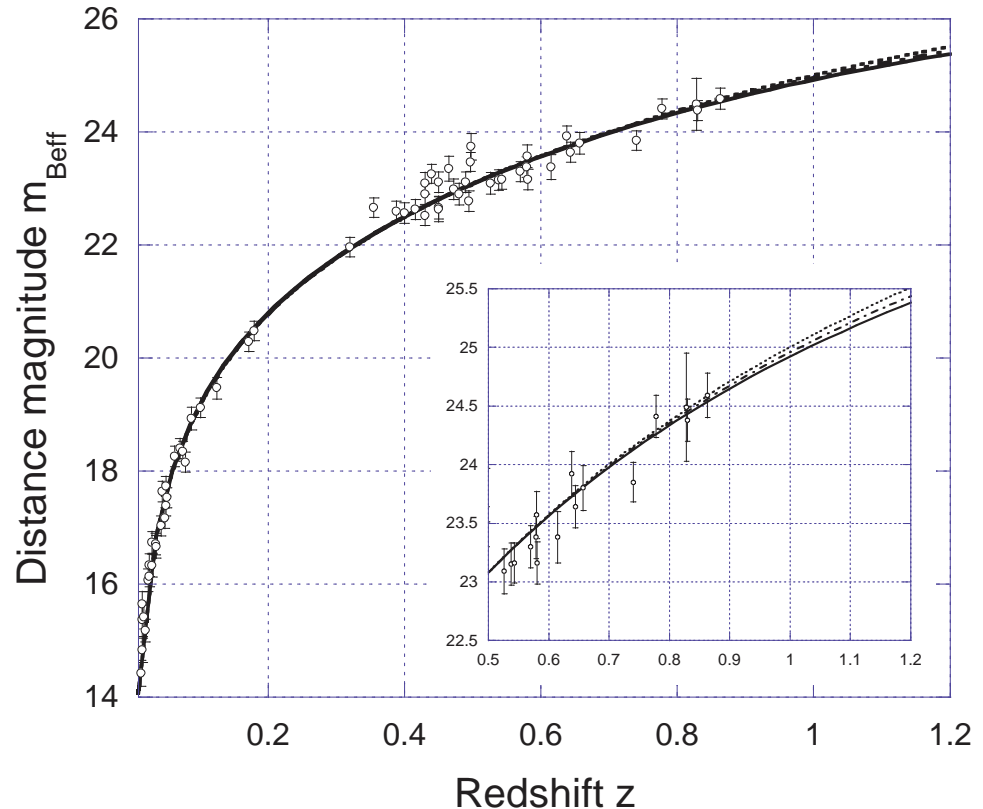


Figure 3: Data taken from Table 5 of Knop *et al* [15]. The solid line curve uses the best fit value of  $a$  with  $\Omega_m = 0.063$ , the dot-dash line curve uses the best fit value of  $a$  with  $\Omega_m = 0.042$  and the dotted line curve uses the best fit value of  $a$  with  $\Omega_m = 0.021$ . An absolute magnitude  $M_B = 19.3$  was assumed in these fits.

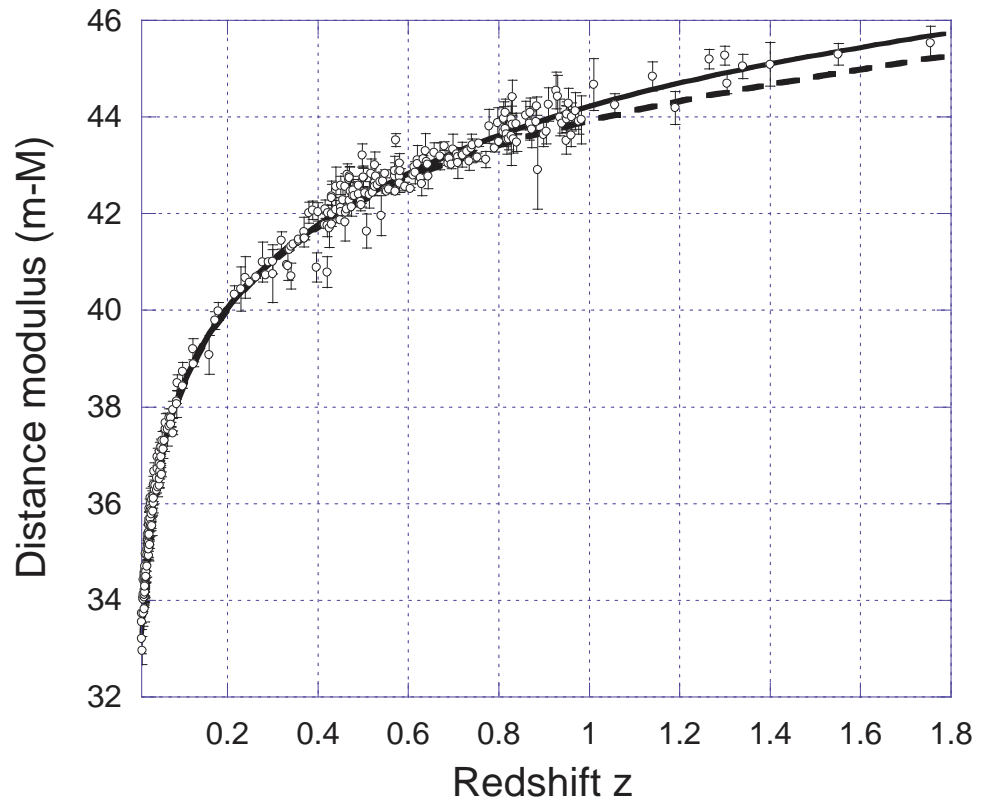


Figure 4: The combined data sets of Riess *et al* and Astier *et al*. The solid line represents the statistically best fit curve with  $a = 0.2284$  and  $\Omega_m = 0.0401$  and the broken line represents the curve with  $a = 0.2284$  and  $\Omega_m = 0.263$

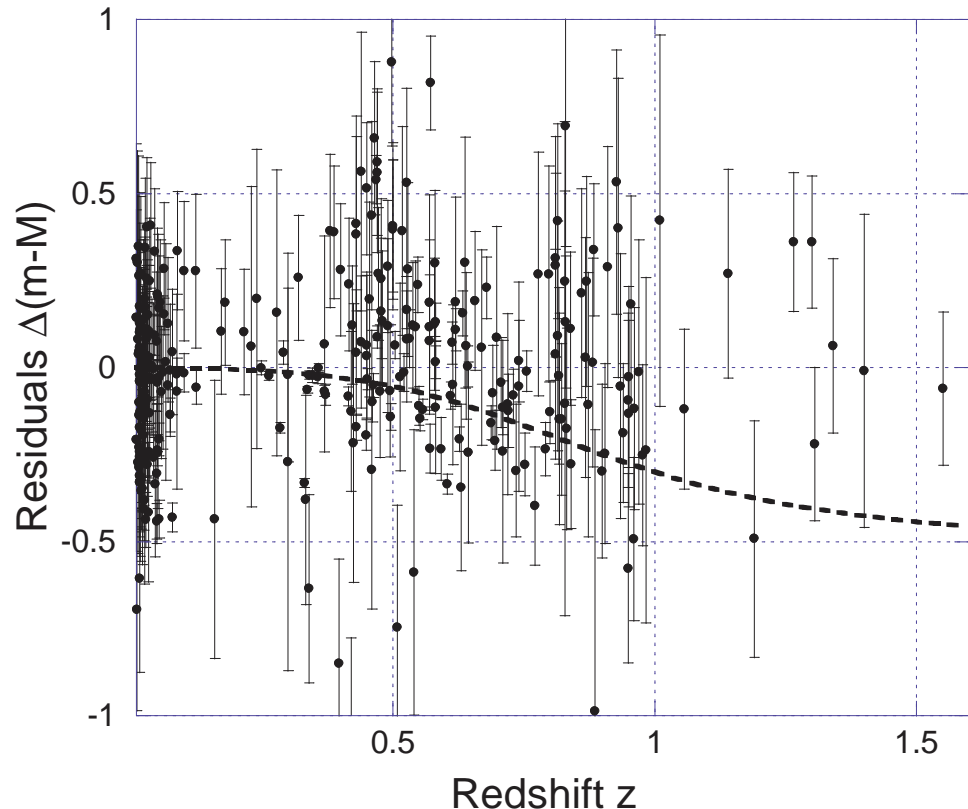


Figure 5: Residuals vs redshift (on linear scale): the differences between the best fit curve with  $\Omega_m = 0.0401$  and  $a = 0.2284$  and the data of fig. 4. The mean of the residuals is  $8.04 \times 10^{-5}$  when all errors are assumed equal and  $-0.0769$  when weighted by published errors. The broken line represents the curve where  $\Omega_m = 0.263$

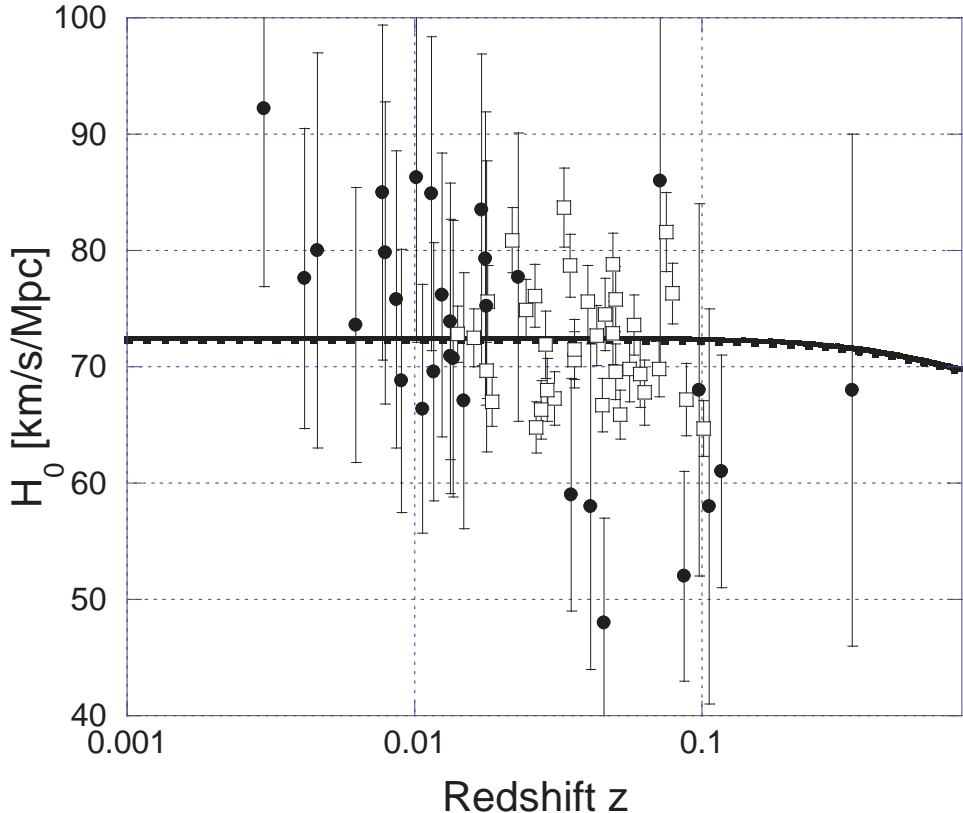


Figure 6: Hubble constant  $H_0$  as a function of redshift,  $z$ . The filled circles are determined from Tully-Fisher measurements taken from [11], Table 5 of [25] and Table 7 of [12], except the point at  $z = 0.333$  is from Sunyaev-Zel'dovich effect taken from Fig. 4 of [25]. The open squares are determined from the SN Ia measurements and taken from Table 6 of [12] and Table 5 of [21]. The errors are those quoted in the sources from which the data was taken

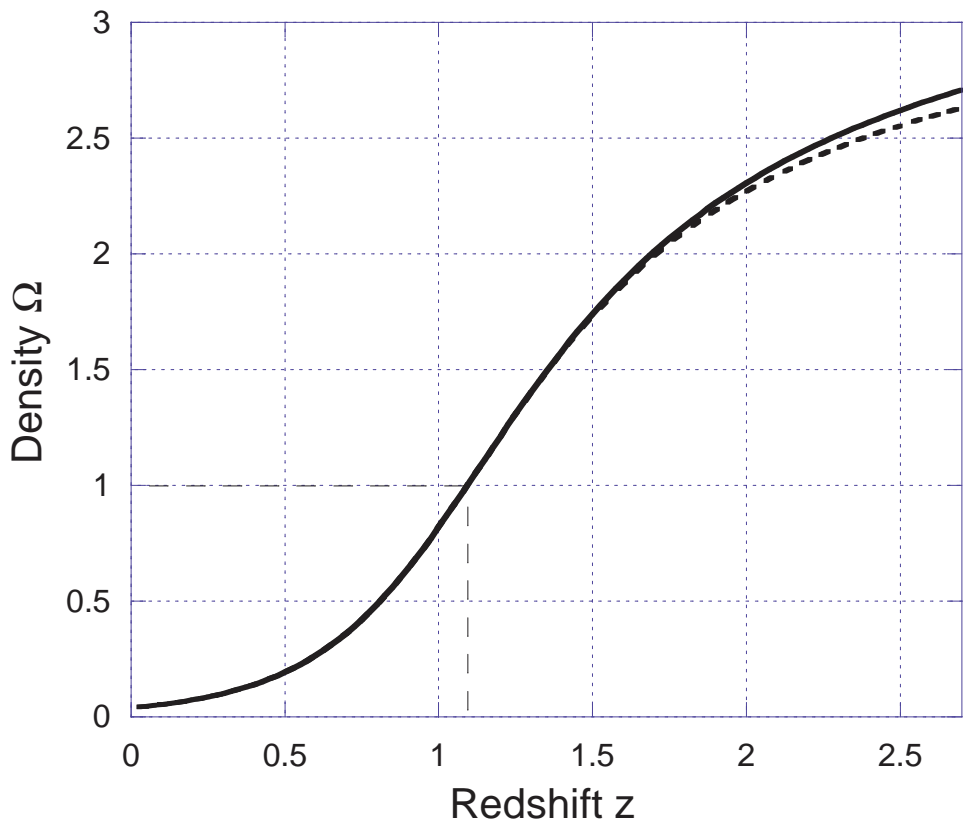


Figure 7: Density model shown as function of redshift for both approximated (broken line) and exact (solid line) with the same value of  $\Omega_m = 0.04$ . The transition redshift  $z_t = 1.095$  where  $\Omega = 1$  is indicated by the dashed lines

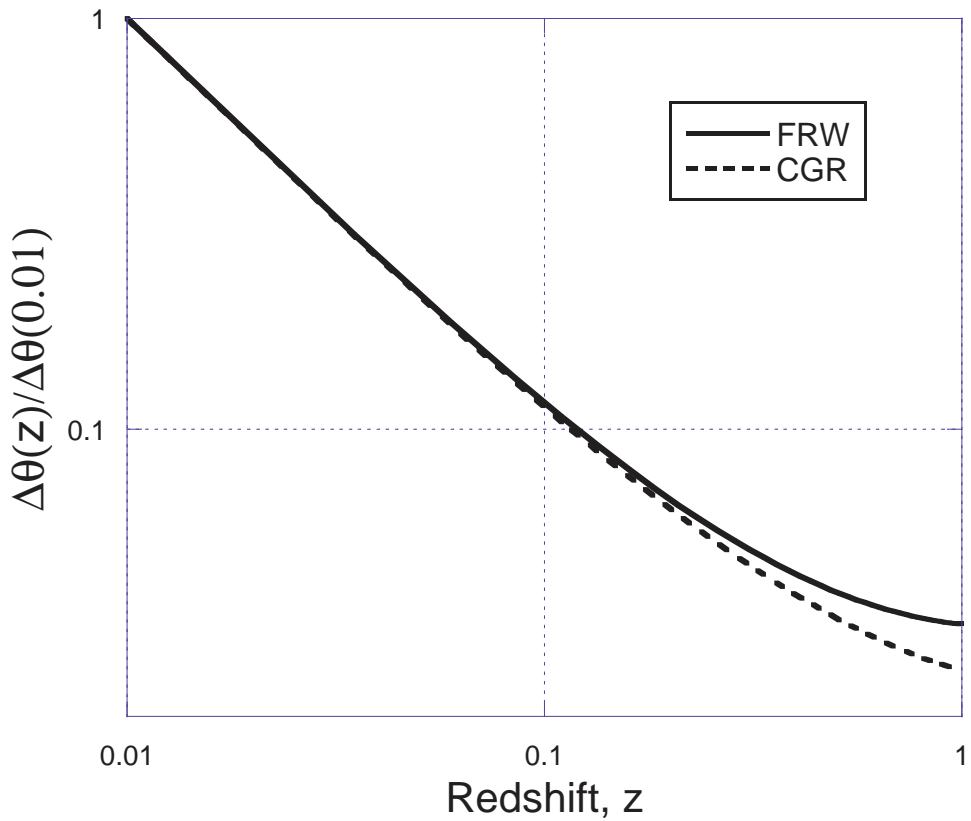


Figure 8: Angular size shown as a function of redshift for both the FRW model (solid line-curve 1) with a deceleration parameter  $q_0 = 1/2$  or  $\Omega_m = 1$  and the CGR model with  $\Omega_m = 0.04$  (broken line-curve 2)